High-Extinction-Ratio and Compact 1310/1550 nm Wavelength Diplexer on SOI Platform Based on an SWG-Structured Two-Mode Interference Coupler

Jinsong Zhang, *Graduate Student Member, IEEE*, Luhua Xu, *Member, IEEE*, Deng Mao, *Graduate Student Member, IEEE*, Zhenping Xing, Yannick D'Mello, Maxime Jacques, Yun Wang, Stephane Lessard, and David V. Plant, *Fellow, IEEE*

***Abstract*—We propose a 1310/1550 nm wavelength diplexer on a 220-nm silicon-on-insulator (SOI) platform. The device is based on a compact two-mode interference (TMI) coupler enabled by a subwavelength grating (SWG) slot. The ideal beat length ratio of 2:1 is achieved with the transverse magnetic (TM) mode by fine-tuning the SWG slot parameters, resulting in a TMI length of only 37 μm. We reveal that the key to high extinction ratio (ER) is the careful design of the tapers, and the device achieves high ERs of 28.05/42.54 dB at 1310/1550 nm with simulation. The measured bandwidths for ER $>$ 15 dB are 82 nm and 56 nm at O- and C-band. Moreover, the design guarantees large calculated 1-dB-insertion-loss (IL) bandwidths of 192/123 nm at 1310/1550 nm. To the best of our knowledge, this is the first experimental demonstration of a high-performance compact silicon 1310/1550 nm diplexer based on a TMI coupler.**

***Index Terms*—Waveguide devices, silicon nanophotonics, subwavelength structures.**

I. Introduction

PHOTONIC integrated circuits (PICs) implemented on the silicon-on-insulator (SOI) platform have attracted a lot of attention in recent years, because they enable dense integration of photonic devices while remaining compatible with complementary metal-oxide-semiconductor (CMOS) processes. Various silicon integrated devices have been developed, including 1310/1550 nm wavelength diplexers, which is an essential part of a passive optical network. Different structures have been proposed for this device, mainly including multimode interference (MMI) couplers [1]–[3], directional couplers (DCs) [4]–[6], and grating couplers [7], [8]. Diplexers based on advanced optimization techniques such as inverse design [9], [10] and particle swarm optimization (PSO) [11] were demonstrated as well.

Among all the designs mentioned above, the MMI coupler stands out because of its low insertion loss (IL) and broad bandwidth [12]. Nevertheless, to realize wavelength multiplexing, the length of the multimode interference section must be a common multiple of the first self-imaging length of both wavelengths. Limited by this requirement, a 1310/1550 nm diplexer based on the MMI usually comes with a large footprint. Efforts have been made to make MMI-based wavelength diplexers more compact, utilizing novel structures such as Bragg gratings [13], photonic crystals (PCs) [14], and subwavelength gratings (SWGs) [15]. The SWG, which can be regarded as a homogeneous material when its pitch is small enough [16], enables more flexible design for integrated photonic devices fabricated using a single etch step. Benefiting from advancing fabrication technologies, the SWG has shown its powerful functionality in various silicon photonic devices over the past decade, such as power splitters [17], microring resonators [18], polarization beam splitters [19], and waveguide crossings [20]. In [15], an SWG slot was introduced in the middle of an MMI coupler to shrink the device length to ˜30% of previously reported designs. A more recent work [21] applied the similar idea to add double SWG slots to the MMI coupler, further reducing the device length. However, both designs were only verified by simulation, and the extinction ratios (ERs) are relatively low.

We propose in this letter the first experimental demonstration of a compact 1310/1550 nm wavelength diplexer based on a two-mode interference (TMI) coupler. The TMI coupler [22] is a special type of MMI coupler in which only two modes are supported in the mode interference section. It has a relatively short coupling length, and it has also been studied on the SOI platform [23]. We show that by inserting an SWG slot in an MMI coupler and a careful design of the tapers, we can realize two-mode interference in the device and consequently reduce the coupling length. The taper design also optimizes the ERs at both ports. As a result, the calculated ERs at 1310 nm and 1550 nm reach 28.05 and 42.54 dB. The proposed design works in the transverse magnetic (TM) mode to achieve the ideal beat length ratio of 2:1, which results in a short coupler length of 37 μm. The device is fabricated on a standard 220-nm SOI platform and then characterized experimentally. The measured results

Manuscript received November 30, 2021; revised February 4, 2022; accepted February 4, 2022. Date of publication February 10, 2022; date of current version February 22, 2022. *(Corresponding author: Jinsong Zhang.)*

Jinsong Zhang, Deng Mao, Zhenping Xing, Yannick D'Mello, Maxime Jacques, Yun Wang, and David V. Plant are with Photonics System Group, Department of Electrical and Computer Engineering, McGill University, Montreal, QC H3A0G4, Canada (e-mail: jinsong.zhang@mail.mcgill.ca; deng.mao@mail.mcgill.ca; zhenping.xing@mail.mcgill.ca; yannick.dmello@mail.mcgill.ca; maxime.jacques@mail.mcgill.ca; oscar.yunwang@gmail.com; david.plant@mcgill.ca).

Luhua Xu is with CMC Microsystems, Kingston, ON H3C 6M8, Canada (e-mail: luhua.xu@cmc.ca).

Stephane Lessard is with Ericsson Canada, Montreal, QC H4S 0B6, Canada (e-mail: stephane.lessard@ericsson.com).

Digital Object Identifier 10.1109/JPHOT.2022.3149998

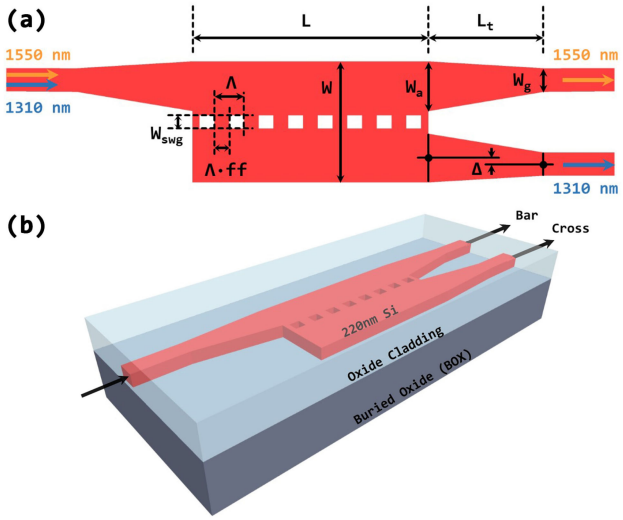

Fig. 1. (a) 2D and (b) 3D schematics of the proposed device.

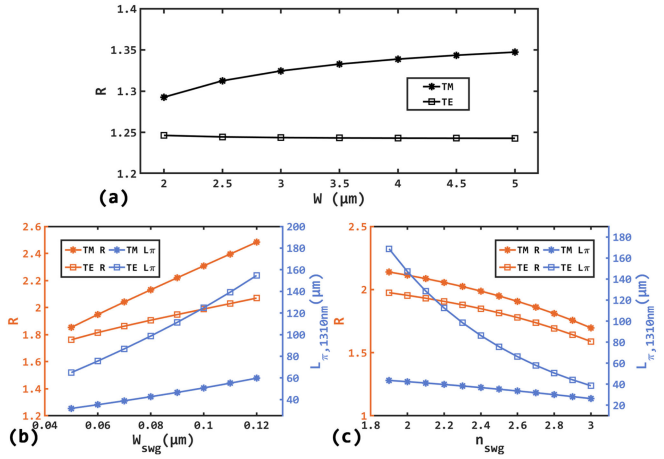

Fig. 2. Calculated beat length ratio, and beat length at $\lambda = 1310$ nm for both the TM and TE modes, as functions of (a) width of the MMI coupler (without the SWG slot), (b) width of the SWG slot and (c) equivalent refractive index of the SWG slot.

also show high performance that the 15-dB-ER bandwidths are 82 nm and 56 nm at O-band and C-band, respectively. As for the IL, the calculated 1-dB-IL bandwidths are 192/123 nm at O/C-bands, which satisfies the International Telecommunication Union (ITU) standard.

II. Design and Analysis

The device schematic is displayed in Fig. 1. The mode interference section has a length of L and a width of W. Compared with regular MMI/TMI couplers, our device has an SWG slot along the direction of light propagation. This slot is placed in the middle with a width of W_{swg}. As a periodic structure, the SWG is described with a pitch Λ and a fill factor ff, so that the lengths of a ridge (Si) and a groove (oxide cladding) in one period are $\Lambda * ff$ and $\Lambda * (1 - ff)$, respectively. Since the gratings need to operate in the subwavelength regime, $\Lambda < \lambda/2n_{eff}$ should be fulfilled at all operating wavelengths. The upper bound of the pitch is about 218 nm at $\lambda = 1310$ nm, thus Λ is preset to 200 nm. In addition, a taper with a length of L_t is utilized to connect the MMI/TMI access port of width W_a to the interconnecting waveguide of width W_g. To minimize the crosstalk at the output ports, we introduce an offset Δ between the centers of the access port and the strip waveguide, as shown in Fig. 1.

In any coupler implementing a mode interference scheme (MMI, DC, TMI), a key step in the design process is to calculate the beat length of the two lowest order modes. This beat length is defined as $L_\pi = \lambda/2/(n_{eff0} - n_{eff1})$. In order to separate the two wavelengths 1310 nm and 1550 nm, the following equation should be satisfied:

$$L_{lcm} = n * L_{\pi,1310} = m * L_{\pi,1550}, \tag{1}$$

where L_{lcm} is the least common multiple of the beat lengths at 1310 nm and 1550 nm, and integers n and m should have different parity (either even and odd, or odd and even). Here we define a beat length ratio $R = L_{\pi,1310}/L_{\pi,1550}$.

Next, the device length L can be determined as:

$$L = a * L_{lcm}, \tag{2}$$

where a is a constant depending on the type of device. a equals 3 for MMI couplers (general interference) whereas the value becomes 1 for DCs and TMI couplers.

To minimize the device length, the values of n and m in (1) should be as small as possible. However, in conventional MMI couplers it is hard to tune the beat length ratio R and achieve certain values of n and m, since the coupler width is the only parameter to adjust. This is illustrated in Fig. 2(a), where we change the width of a conventional MMI coupler without any slot and calculate the corresponding beat length ratio for both the TE and TM modes. Here we use the finite-difference eigenmode (FDE) solver for the mode effective index calculation. The result indicates that the ratio is relatively solid near 1.25 with the TE mode so that $m = 5, n = 4$, leading to a long interference section. In the case of the TM mode, the ratio is close to 1.33 implying $m = 4, n = 3$, which are still large values.

Therefore we insert an SWG slot in an MMI coupler to adjust the beat length ratio with more degrees of freedom. First, we replace the SWG with a homogeneous material with index n_{swg} based on the effective medium theory, so that the 2D analysis using FDE solver is enabled. Initially we conduct a parameter sweep on W_{swg}, assuming n_{swg} is 2.5 and W is 2.5 μm. Then we plot the beat lengths at $\lambda = 1310$ nm, as well as the ratio R in Fig. 2(b). The reason we select $W = 2.5$ μm is that W should be large enough to avoid crosstalk between the two output single-mode waveguides, whilst on the other hand, W should be as small as possible so that the coupler length is minimized. Hence, $W = 2.5$ μm is a proper choice. As a result, $R_{TM} \approx 2$ is achieved at $W_{swg} = 0.06$ μm, whereas $R_{TE} \approx 1.8$. With $R = 2$ the values of m, n are actually minimized to $m = 2, n = 1$, which is the ideal case. Although we can realize this target ratio with the TE mode as well by increasing W_{swg}, the beat length almost triples compared with the TM mode. Meanwhile, since the minimum feature size of the fabrication process we plan

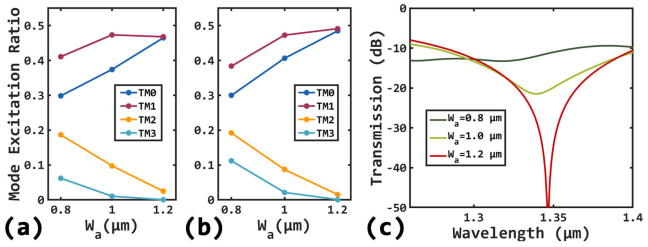

Fig. 3. Calculated power distributions of the TM modes excitation under different access port widths W_a, at (a) $\lambda = 1550$ nm and (b) $\lambda = 1310$ nm. (c) Dependence of transmission spectra on W_a.

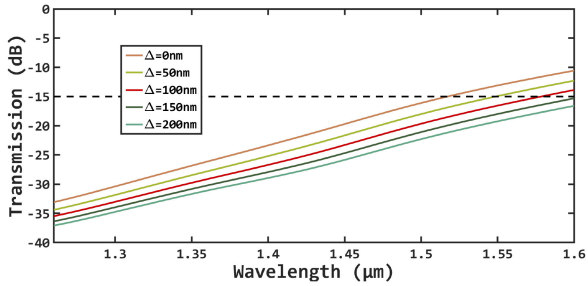

Fig. 4. Calculated crosstalk between bar and cross ports as a function of wavelength, under various values of offset Δ.

to use is 0.06 μm, we fix $W_{swg} = 0.06$ μm because it provides the smallest beat length. Then we optimize n_{swg}. Similarly in Fig. 2(c) where the ratio is plotted as a function of n_{swg} with the fixed $W_{swg} = 0.06$ μm, $R_{TE} = 2$ can only be reached with $n_{swg} \approx 1.9$ at the cost of a large beat length. Thus, we choose the TM mode to be the operating mode for a more compact design. As shown in Fig. 2(c) the optimal value of n_{swg} is 2.4. This value will be used for estimating the fill factor ff in the post 3D simulation analysis where we use the actual SWG structures.

The next step is to design the taper. Normally the taper design rule for MMI couplers is simple, i.e. the access port should be wide enough and we need large intervals between ports to compress the crosstalk. However, the taper needs to be carefully examined in our device since it fundamentally affects its working principle. It is revealed that increasing the access port width W_a in a slotted MMI coupler reduces the excitation of higher-order modes, leaving only TM0 and TM1 modes. To verify this, we perform 3D finite-difference time-domain (FDTD) simulations in which we set up a mode expansion monitor in the mode interference section to calculate the proportion of each excited mode in terms of power. The width of the interconnecting single-mode waveguide is set to $W_g = 350$ nm to meet the single-mode condition for the O-band. The offset Δ is set to 0 temporarily, and the taper length is preset to $L_t = 9$ μm, which is long enough to avoid the excitation of high-order TM modes at the access ports. As shown in Fig. 3(a) and (b), increasing the port width to $W_a = 1.2$ μm effectively reduces the excitation of TM2 and higher-order modes. With only TM0 and TM1 modes being equally excited, the device functions as a TMI coupler instead of an MMI coupler. Therefore, the value of a in equation (2) will be 1 rather than 3, resulting in a much smaller device length. We draw several bar port transmission spectra of a sample device with an arbitrary length in Fig. 3(c) as we change W_a, and we observe that a large value of W_a is the key to effective device performance. Such design result in the high ER of the proposed wavelength diplexer.

Since $L = a * n * L_{\pi,1310}$, our design reduces the coefficient $a * n$ by a factor of 9. Although the beat length of a regular MMI coupler with the same width at $\lambda = 1.31$ μm is ˜43% of that in our device, the device length is still shortened by a factor of 3.87.

Since a much wider access port is applied, the crosstalk between the bar and the cross ports is no longer negligible, which will cause the transmission spectrum to shift. Our solution to this problem is to create an offset Δ for the interconnecting waveguides on the y-axis, as illustrated in Fig. 1(a). 3D FDTD simulations are again performed to calculate the crosstalk with different Δ. However, the simulation model applied here is different, where the coupler part is removed and only the two output waveguides and tapers are considered. With the top interconnecting waveguide being the input port, we calculate the transmission through the bottom access port as the crosstalk. The results are shown in Fig. 4. The crosstalk cannot be fully eliminated due to the relatively large access port width. Nonetheless, since the TMI coupler works as a DC under this scheme, we can regard the TMI coupler and the taper section as two cascaded DCs. As long as we compress the crosstalk to an insignificant amount, we can always recover the intended transmission spectrum by slightly tuning the length of the TMI coupler. As a result, we set Δ to 0.1 μm so that the crosstalk at $\lambda = 1310$ nm and $\lambda = 1550$ nm are both below -15 dB, which is insignificant enough.

The other device geometries, including fill factor ff and TMI length L, are determined by performing a joint parameter sweep analysis using 3D FDTD simulations as mentioned above, where we replace the homogeneous material with a real SWG. We use Rytov's formulas [24] to estimate the ff that corresponds to the theoretical value of n_{swg} (2.4), as the start point of the joint sweep. Then we calculate $L = L_{\pi,1310}$ under each ff as the reference for choosing lengths in the sweep. In Fig. 5, we show the featured transmission spectra under 3 fill factors $ff = 0.30, ff = 0.37, ff = 0.44$, each with 5 different TMI lengths. According to the results, the device length and fill factor of the SWG are determined as $L = 37$ μm and $ff = 0.37$, respectively, under which the transmission spectra of the two output ports have minimum points at the target wavelengths. Quantitatively analyzing, we define the figure of merit (FOM) of the optimization as the summation of the transmission (in dB) through the bar port at $\lambda = 1310$ nm and the transmission (in dB) through the cross port at $\lambda = 1550$ nm, and we need to minimize the FOM. With the combination of $L = 37$ μm and $ff = 0.37$, the FOM reaches -71.16 dB, which is the minimum value among all the parameter pairs shown in Fig. 5.

IL and ER are commonly used metrics for these types of devices, which are defined as:

$$\text{IL} = 10 * \log_{10}(P_{in}/P_{out}), \tag{3}$$

$$\text{ER} = 10 * \log_{10}(P_{out}/P'_{out}), \tag{4}$$

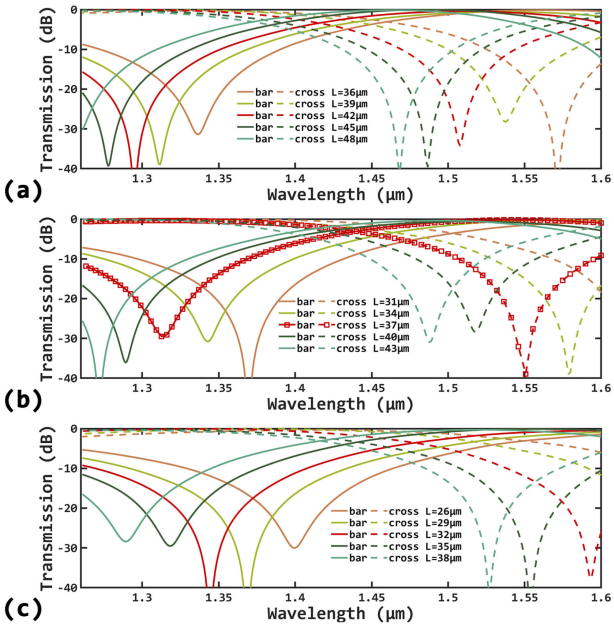

Fig. 5. Simulated transmission spectra of both bar and cross ports under different TMI length L at (a) $ff = 0.30$, (b) $ff = 0.37$ and (c) $ff = 0.44$. The optimized spectrum is the emphasized red curve with markers in (b).

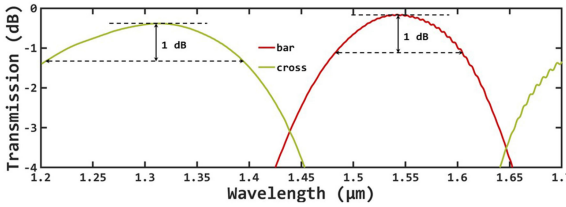

Fig. 6. Magnified transmission spectra of the bar and cross ports with the optimal parameters. This figure illustrates the 1-dB-IL bandwidths at both ports.

where P_{out} is the optical power of the corresponding output port for a particular wavelength (bar for 1550 nm and cross for 1310 nm), and P'_{out} is the power of the other output port (cross for 1550 nm and bar for 1310 nm). P_{in} stands for the input power. The simulation results indicate that the values of IL and ER are 0.36 dB and 28.05 dB at $\lambda = 1310$ nm, respectively, and 0.21 dB and 42.54 dB at $\lambda = 1550$ nm, respectively. As illustrated in Fig. 6, the 1-dB-IL bandwidth at O-band is as wide as 192 nm from 1203 nm to 1395 nm. To the best of our knowledge, this is one of the largest values that are reported. Such a wide band may stem from the beat length ratio of 1:2, under which there is no spectral peak at shorter wavelengths than 1310 nm. Therefore the IL declines slowly around the O-band. As for the C-band, the 1-dB-IL bandwidth is 123 nm from 1482 nm to 1605 nm, which also meets the ITU standard. For the ER bandwidth, we use 15 dB as the criteria, which ensures that the signal at the unwanted wavelength can be attenuated to a level that will not severely distort the signal being transmitted. As a result, ER $>$ 15 dB is achieved within a 65 nm range and a 50 nm range in the O-band and the C-band respectively. Mode evolution at both wavelengths are demonstrated in Fig. 7, where we can clearly observe the ideal beat length ratio of $m/n = 2/1$.

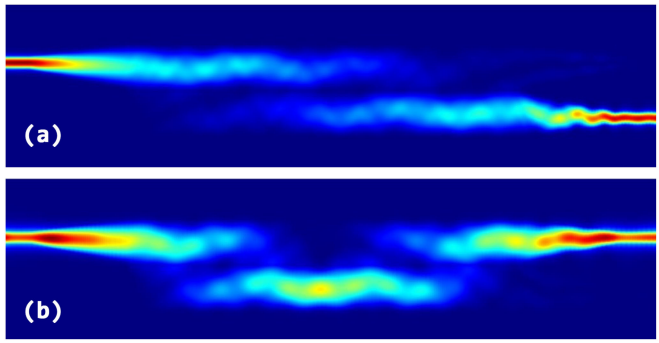

Fig. 7. Calculated mode evolution (power density distribution) of the proposed device at (a) $\lambda = 1310$ nm and (b) $\lambda = 1550$ nm.

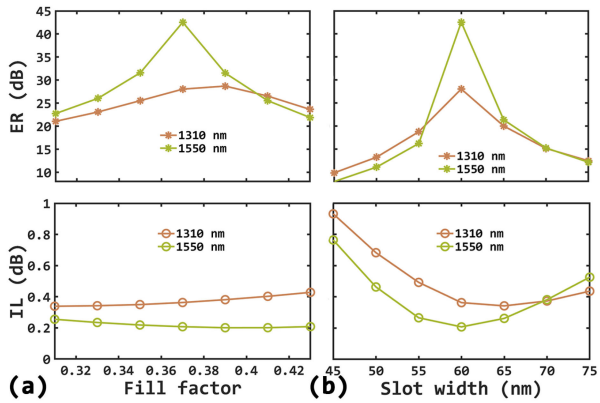

Fig. 8. Dependence of the ILs and ERs on (a) the fill factor and (b) the SWG slot width.

Fabrication tolerance tends to be an problem for devices with fine features such as SWG. As for our proposed device, we analyze the impact of the slot width W_{swg} and the fill factor ff. As demonstrated in Fig. 8(a), even with a fill factor ranging from (0.31,0.43), the ILs at both ports do not exceed 0.45 dB, and the values of ER are maintained above 20 dB. Since the fill factors of gratings are likely to drift in fabrication, such results prove the robustness of our SWG-based design. Fig. 8(b) shows that the width change of the SWG slot from 60 nm to 45 nm reduces the ER to 9.85 dB at 1310 nm and 7.80 dB at 1550 nm, whereas the values of IL are kept below 1 dB at both ports. Hence, the SWG slot width should be the main parameter to be controlled in the tape-out process. On the other hand, The minuscule holes in the SWG slot may cause imperfect filling of the cladding. Therefore, we simulate the same structure without silica deposited into the holes to evaluate the influence of this effect. It is revealed by simulation that even with such an extreme model, the ILs and ERs at 1310/1550 nm achieve 0.33/0.23 dB and 21.31/25.72 dB, justifying that the impact is not fatal at all.

III. Fabrication and Characterization

The device is fabricated using the NanoSOI fabrication process provided by Applied Nanotools Inc. The chip has a 220-nm-thick Si layer on a 2-μm-thick buried oxide layer, with a 2.2-μm-thick cladding oxide on top. As for the testing setup,

TABLE I
PERFORMANCE COMPARISON WITH PREVIOUSLY REPORTED 1310/1550 nm WAVELENGTH DIPLEXERS ON THE SOI PLATFORM

Reference	Structure	1-dB-IL BW (nm)		ER (dB)		15-dB-ER BW (nm)		Length (μm)	Polarization	Method
		O-band	C-band	1310 nm	1550 nm	O-band	C-band			
[4]	DC	/	/	25.67	14.89	~40	~35	48.2	TE&TM	Simulation
[5]	DC	/	/	27.07	25.84	>80	~70	150 (triplexer)	TE	Experiment
[6]	DC	140	125	~15	~23	/	/	13.5	TE	Simulation
[14]	MMI	/	/	32.60	16.40	74	103	108.5	TE	Experiment
[15]	MMI	150	120	22.18	20.10	/	/	43.4	TE	Simulation
[21]	MMI	>90	>90	15.20	16.80	/	/	34.5	/	Simulation
This work	TMI	192	123	28.05	42.54	65	50	37	TM	Simulation
This work	TMI	/	/	19.58	26.56	82	56	37	TM	Experiment

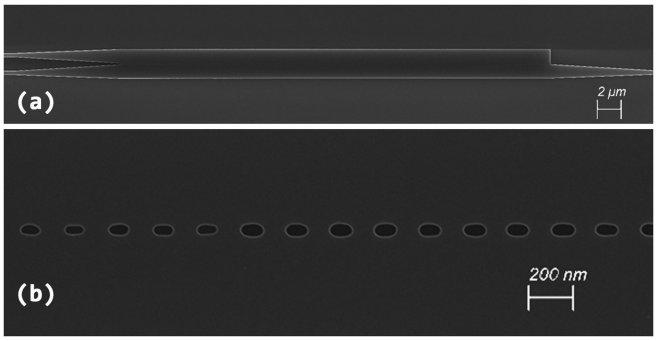

Fig. 9. SEM images of (a) the wavelength diplexer and (b) the SWG slot.

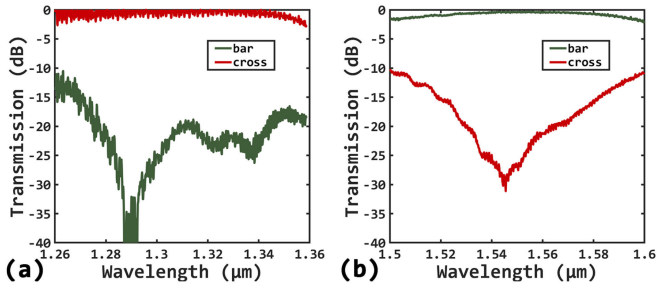

Fig. 10. Measured transmission spectra in (a) the O-band (1260 nm - 1360 nm) and (b) the C-band (1500 nm - 1600 nm).

we use grating couplers with a broadband design [25], [26] to guide the light between the chip and the fiber array. The light sources are the Yenista TUNICS T100S-HP O-band and C-band tunable lasers, assisted by a Yenista CT400 passive optical component tester to conduct efficient measurements. Since the grating couplers are designed only for either the O-band or the C-band, the proposed 1310/1550 nm diplexer is fabricated in pairs connected to different grating couplers, so that we can obtain the transmission spectra of both bands for the same structure. Grating coupler pairs that are connected directly are fabricated alongside the devices for data normalization. A polarization controller is inserted between the laser and the device to maximize the power of the TM-polarized light.

The images from the scanning electron microscope (SEM) are displayed in Fig. 9, which shows that the on-chip SWG slot has been successfully constructed. The power transmission spectra in both the O-band and the C-band are displayed in Fig. 10. The measured IL and ER at $\lambda = 1310$ nm are 0.33 dB and 19.58 dB, respectively, whereas the values at $\lambda = 1550$ nm are 0.45 dB and 26.56 dB, respectively. The experimental results differ from the simulation results that the minimum point of the O-band transmission spectrum in the bar port is not located at 1310 nm (it is shifted by approximately 20 nm). However, the device still demonstrates excellent properties in terms of bandwidth. The fabricated device achieves an ER higher than 15 dB over an 82-nm wavelength range in the O-band from 1277 nm to 1359 nm, and a 56-nm range in the C-band from 1525 nm to 1581 nm. Since oscillations are observed in the measured spectra, especially in the O-band, it is hard to characterize the 1-dB-IL bandwidth. Nevertheless, even with the defect, the measured IL is less than 2 dB within an 88-nm bandwidth in the O-band from 1266 nm to 1354 nm, and a 99-nm bandwidth in the C-band from 1500 nm to 1599 nm.

In Table I, we compare the performances of various reported silicon 1310/1550 nm wavelength diplexers based on similar principles (DC, MMI). It is shown that our proposed design exhibits high ER and wide bandwidths in terms of both IL and ER. Furthermore, the device achieves one of the shortest length among experimentally verified counterparts.

IV. CONCLUSION

In conclusion, we propose and experimentally verify a novel TMI-coupler-based high-performance 1310/1550 nm diplexer on a standard 220-nm SOI platform. It is shown that the insertion of an SWG and an appropriate design of the tapers make an MMI coupler operate in a two-mode interference scheme that reduces the device length while maintaining high ER. Meanwhile the device achieves an ideal beat length ratio of 2:1 for the two target wavelengths using the TM mode, which makes the device more compact with a TMI coupler length of only 37 μm. With 3D FDTD simulations, the proposed diplexer achieves 1-dB-IL bandwidths larger than 120 nm and 15-dB-ER bandwidths larger than 50 nm at both ports. As for the peak values, the calculated ERs at 1310 nm and 1550 nm reach 28.05 dB and 42.54 dB, respectively. The measured results of the fabricated device indicate that ILs at $\lambda = 1310$ nm and $\lambda = 1550$ nm are 0.33 dB and 0.45 dB, respectively. Measured 15-dB-ER bandwidths of 82 nm and 56 nm are accomplished in the O-band and the C-band, respectively, and the ER reaches 19.58 dB at $\lambda = 1310$ nm and 26.56 dB at $\lambda = 1550$ nm. Analysis of fabrication tolerance is conducted, and the results prove that the proposed structure is rather insensitive to the fluctuation of the SWG fill factor, which eases the optimization in the fabrication process.

ACKNOWLEDGMENT

The authors would like to acknowledge Lumerical Inc. and CMC Microsystems for providing design tools, and Applied Nanotools Inc. for fabricating the device.

REFERENCES

[1] J. Xiao, X. Liu, and X. Sun, "Design of an ultracompact MMI wavelength demultiplexer in slot waveguide structures," *Opt. Exp.*, vol. 15, no. 13, pp. 8300–8308, 2007.

[2] Y. Shi, S. Anand, and S. He, "A polarization-insensitive 1310/1550-nm demultiplexer based on sandwiched multimode interference waveguides," *IEEE Photon. Technol. Lett.*, vol. 19, no. 22, pp. 1789–1791, Nov. 2007.

[3] J. Chen, P. Liu, and Y. Shi, "An on-chip silicon compact triplexer based on cascaded tilted multimode interference couplers," *Opt. Commun.*, vol. 410, pp. 483–487, 2018.

[4] Y. Shi, S. Anand, and S. He, "Design of a polarization insensitive triplexer using directional couplers based on submicron silicon rib waveguides," *J. Lightw. Technol.*, vol. 27, no. 11, pp. 1443–1447, 2009.

[5] H. Xu and Y. Shi, "On-chip silicon triplexer based on asymmetrical directional couplers," *IEEE Photon. Technol. Lett.*, vol. 29, no. 15, pp. 1265–1268, Aug. 2017.

[6] J. Chen, "A broadband wavelength demultiplexer assisted by SWG-based directional couplers," *Optik*, vol. 202, 2020, Art. no. 163602.

[7] G. Roelkens, D. Van Thourhout, and R. Baets, "Silicon-on-insulator ultra-compact duplexer based on a diffractive grating structure," *Opt. Exp.*, vol. 15, no. 16, pp. 10 091–10 096, 2007.

[8] C. R. Doerr, L. Chen, M. S. Rasras, Y.-K. Chen, J. S. Weiner, and M. P. Earnshaw, "Diplexer with integrated filters and photodetector in Ge–Si using $\Gamma - X$ and $\Gamma - M$ directions in a grating coupler," *IEEE Photon. Technol. Lett.*, vol. 21, no. 22, pp. 1698–1700, Nov. 2009.

[9] A. Y. Piggott, J. Lu, T. M. Babinec, K. G. Lagoudakis, J. Petykiewicz, and J. Vučković, "Inverse design and implementation of a wavelength demultiplexing grating coupler," *Sci. Rep.*, vol. 4, 2014, Art. no. 7210.

[10] A. Y. Piggott, J. Lu, K. G. Lagoudakis, J. Petykiewicz, T. M. Babinec, and J. Vučković, "Inverse design and demonstration of a compact and broadband on-chip wavelength demultiplexer," *Nat. Photon.*, vol. 9, no. 6, pp. 374–377, 2015.

[11] Y. Ma, P. Magill, T. Baehr-Jones, and M. Hochberg, "Design and optimization of a novel silicon-on-insulator wavelength diplexer," *Opt. Exp.*, vol. 22, no. 18, pp. 21 521–21 528, 2014.

[12] L. B. Soldano and E. C. M. Pennings, "Optical multi-mode interference devices based on self-imaging: Principles and applications," *J. Lightw. Technol.*, vol. 13, no. 4, pp. 615–627, 1995.

[13] J. Chen, Y. Zhang, and Y. Shi, "An on-chip triplexer based on silicon Bragg grating-assisted multimode interference couplers," *IEEE Photon. Technol. Lett.*, vol. 29, no. 1, pp. 63–65, Jan. 2017.

[14] L. Xu *et al.*, "Broadband 1310/1550 nm wavelength demultiplexer based on a multimode interference coupler with tapered internal photonic crystal for the silicon-on-insulator platform," *Opt. Lett.*, vol. 44, no. 7, pp. 1770–1773, 2019.

[15] L. Liu, Q. Deng, and Z. Zhou, "An ultra-compact wavelength diplexer engineered by subwavelength grating," *IEEE Photon. Technol. Lett.*, vol. 29, no. 22, pp. 1927–1930, Nov. 2017.

[16] R. Halir *et al.*, "Waveguide sub-wavelength structures: A review of principles and applications," *Laser Photon. Rev.*, vol. 9, no. 1, pp. 25–49, 2015.

[17] L. Xu *et al.*, "Compact high-performance adiabatic 3-dB coupler enabled by subwavelength grating slot in the silicon-on-insulator platform," *Opt. Exp.*, vol. 26, no. 23, pp. 29873–29885, 2018.

[18] V. Donzella, A. Sherwali, J. Flueckiger, S. M. Grist, S. T. Fard, and L. Chrostowski, "Design and fabrication of SOI micro-ring resonators based on sub-wavelength grating waveguides," *Opt. Exp.*, vol. 23, no. 4, pp. 4791–4803, 2015.

[19] L. Xu *et al.*, "Polarization beam splitter based on MMI coupler with SWG birefringence engineering on SOI," *IEEE Photon. Technol. Lett.*, vol. 30, no. 4, pp. 403–406, Feb. 2018.

[20] P. J. Bock *et al.*, "Subwavelength grating crossings for silicon wire waveguides," *Opt. Exp.*, vol. 18, no. 15, pp. 16146–16155, 2010.

[21] F. Wang, X. Xu, C. Sun, and J. Zhao, "Ultracompact 1310/1550 nm wavelength demultiplexer based on subwavelength grating-assisted multimode interference coupler," *Opt. Eng.*, vol. 60, no. 8, 2021, Art. no. 087104.

[22] F. Rottmann, A. Neyer, W. Mevenkamp, and E. Voges, "Integrated-optic wavelength multiplexers on lithium niobate based on two-mode interference," *J. Lightw. Technol.*, vol. 6, no. 6, pp. 946–952, 1988.

[23] B.-K. Yang, S.-Y. Shin, and D. Zhang, "Ultrashort polarization splitter using two-mode interference in silicon photonic wires," *IEEE Photon. Technol. Lett.*, vol. 21, no. 7, pp. 432–434, Apr. 2009.

[24] S. M. Rytov, "Electromagnetic properties of a finely stratified medium," *Sov. Phys. JETP*, vol. 2, no. 3, pp. 466–475, 1956.

[25] Y. Wang *et al.*, "Design of broadband subwavelength grating couplers with low back reflection," *Opt. Lett.*, vol. 40, no. 20, pp. 4647–4650, 2015.

[26] Y. Wang *et al.*, "Compact single-etched sub-wavelength grating couplers for O-band application," *Opt. Exp.*, vol. 25, no. 24, pp. 30 582–30 590, 2017.